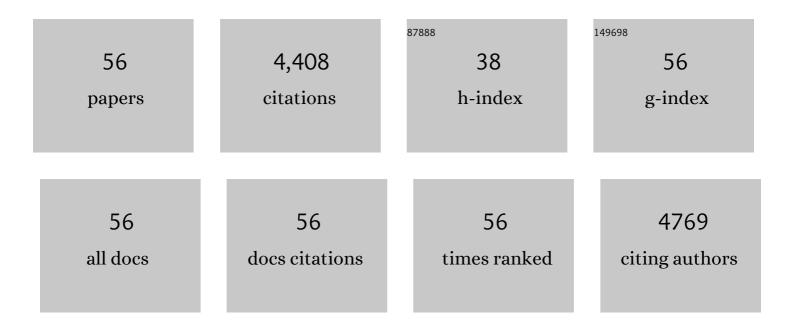
## Kathryn L Nagy

List of Publications by Year in descending order

Source: https://exaly.com/author-pdf/4788141/publications.pdf Version: 2024-02-01



#	Article	IF	CITATIONS
1	Acute Toxicity of Divalent Mercury to Bacteria Explained by the Formation of Dicysteinate and Tetracysteinate Complexes Bound to Proteins in <i>Escherichia coli</i> and <i>Bacillus subtilis</i> . Environmental Science & Technology, 2021, 55, 3612-3623.	10.0	9
2	Demethylation of Methylmercury in Bird, Fish, and Earthworm. Environmental Science & Technology, 2021, 55, 1527-1534.	10.0	61
3	Divalent Mercury in Dissolved Organic Matter Is Bioavailable to Fish and Accumulates as Dithiolate and Tetrathiolate Complexes. Environmental Science & Technology, 2019, 53, 4880-4891.	10.0	30
4	Effect of pH on the Formation of Gibbsite-Layer Films at the Muscovite (001)–Water Interface. Journal of Physical Chemistry C, 2019, 123, 6560-6571.	3.1	14
5	Thiols in Natural Organic Matter: Molecular Forms, Acidity, and Reactivity with Mercury(II) from First-Principles Calculations and High Energy-Resolution X-ray Absorption Near-Edge Structure Spectroscopy. ACS Earth and Space Chemistry, 2019, 3, 2795-2807.	2.7	9
6	Dissolution Kinetics of Epitaxial Cadmium Carbonate Overgrowths on Dolomite. ACS Earth and Space Chemistry, 2019, 3, 212-220.	2.7	3
7	Evolution of Strain in Heteroepitaxial Cadmium Carbonate Overgrowths on Dolomite. Crystal Growth and Design, 2018, 18, 2871-2882.	3.0	6
8	Heteroepitaxial growth of cadmium carbonate at dolomite and calcite surfaces: Mechanisms and rates. Geochimica Et Cosmochimica Acta, 2017, 205, 360-380.	3.9	28
9	Spatial Dependence of Reduced Sulfur in Everglades Dissolved Organic Matter Controlled by Sulfate Enrichment. Environmental Science & Technology, 2017, 51, 3630-3639.	10.0	78
10	Real-time observation of cation exchange kinetics and dynamics at the muscovite-water interface. Nature Communications, 2017, 8, 15826.	12.8	61
11	Nucleation of mercury sulfide by dealkylation. Scientific Reports, 2016, 6, 39359.	3.3	21
12	Mercury transformation and release differs with depth and time in a contaminated riparian soil during simulated flooding. Geochimica Et Cosmochimica Acta, 2016, 176, 118-138.	3.9	50
13	Chemical Forms of Mercury in Human Hair Reveal Sources of Exposure. Environmental Science & Technology, 2016, 50, 10721-10729.	10.0	53
14	Structural Characterization of Aluminum (Oxy)hydroxide Films at the Muscovite (001)–Water Interface. Langmuir, 2016, 32, 477-486.	3.5	14
15	Fish Consumption and Hair Mercury Among Asians in Chicago. Journal of Occupational and Environmental Medicine, 2015, 57, 1325-1330.	1.7	9
16	Structure, Bonding, and Stability of Mercury Complexes with Thiolate and Thioether Ligands from High-Resolution XANES Spectroscopy and First-Principles Calculations. Inorganic Chemistry, 2015, 54, 11776-11791.	4.0	57
17	Comment on "Molecular controls on Cu and Zn isotopic fractionation in Fe–Mn crusts―by Little et al Earth and Planetary Science Letters, 2015, 411, 310-312.	4.4	9
18	Formation of Mercury Sulfide from Hg(II)–Thiolate Complexes in Natural Organic Matter. Environmental Science & Technology, 2015, 49, 9787-9796.	10.0	111

KATHRYN L NAGY

#	Article	IF	CITATIONS
19	Incorporation of Pb at the Calcite (104)–Water Interface. Environmental Science & Technology, 2014, 48, 9263-9269.	10.0	46
20	Thlaspi arvense binds Cu(ii) as a bis-(l-histidinato) complex on root cell walls in an urban ecosystem. Metallomics, 2013, 5, 1674.	2.4	17
21	Changes in adsorption free energy and speciation during competitive adsorption between monovalent cations at the muscovite (001)-water interface. Geochimica Et Cosmochimica Acta, 2013, 123, 416-426.	3.9	57
22	Monovalent Ion Adsorption at the Muscovite (001)–Solution Interface: Relationships among Ion Coverage and Speciation, Interfacial Water Structure, and Substrate Relaxation. Langmuir, 2012, 28, 8637-8650.	3.5	128
23	Quantitative analysis of sulfur functional groups in natural organic matter by XANES spectroscopy. Geochimica Et Cosmochimica Acta, 2012, 99, 206-223.	3.9	146
24	Metallothionein-Like Multinuclear Clusters of Mercury(II) and Sulfur in Peat. Environmental Science & Technology, 2011, 45, 7298-7306.	10.0	59
25	Heavy Metal Sorption at the Muscovite (001)–Fulvic Acid Interface. Environmental Science & Technology, 2011, 45, 9574-9581.	10.0	35
26	Hydrated Cation Speciation at the Muscovite (001)â^'Water Interface. Langmuir, 2010, 26, 16647-16651.	3.5	126
27	Competitive adsorption of strontium and fulvic acid at the muscovite–solution interface observed with resonant anomalous X-ray reflectivity. Geochimica Et Cosmochimica Acta, 2010, 74, 1762-1776.	3.9	47
28	Enhanced Uptake and Modified Distribution of Mercury(II) by Fulvic Acid on the Muscovite (001) Surface. Environmental Science & Technology, 2009, 43, 5295-5300.	10.0	43
29	Fulvic Acid Sorption on Muscovite Mica as a Function of pH and Time Using In Situ X-ray Reflectivity. Langmuir, 2008, 24, 7817-7829.	3.5	19
30	Thermodynamics, Interfacial Structure, and pH Hysteresis of Rb <sup>+</sup> and Sr <sup>2+</sup> Adsorption at the Muscovite (001)â^'Solution Interface. Langmuir, 2008, 24, 13993-14004.	3.5	58
31	Reaction pathways for quartz dissolution determined by statistical and graphical analysis of macroscopic experimental data. Geochimica Et Cosmochimica Acta, 2008, 72, 4521-4536.	3.9	50
32	Formation of Metallic Copper Nanoparticles at the Soilâ^'Root Interface. Environmental Science & Technology, 2008, 42, 1766-1772.	10.0	221
33	Relationships between Hg(ii)–S bond distance and Hg(ii) coordination in thiolates. Dalton Transactions, 2008, , 1421.	3.3	73
34	Distribution of barium and fulvic acid at the mica–solution interface using in-situ X-ray reflectivity. Geochimica Et Cosmochimica Acta, 2007, 71, 5763-5781.	3.9	53
35	Resonant anomalous X-ray reflectivity as a probe of ion adsorption at solid–liquid interfaces. Thin Solid Films, 2007, 515, 5654-5659.	1.8	30
36	The effect of Al(OH)4â^ on the dissolution rate of quartz. Geochimica Et Cosmochimica Acta, 2006, 70, 290-305.	3.9	114

KATHRYN L NAGY

#	Article	IF	CITATIONS
37	Cation sorption on the muscovite (001) surface in chloride solutions using high-resolution X-ray reflectivity. Geochimica Et Cosmochimica Acta, 2006, 70, 3549-3565.	3.9	182
38	Transient and quasi-steady-state dissolution of biotite at 22–25°C in high pH, sodium, nitrate, and aluminate solutions. Geochimica Et Cosmochimica Acta, 2005, 69, 399-413.	3.9	30
39	Dissolution of cinnabar (HgS) in the presence of natural organic matter. Geochimica Et Cosmochimica Acta, 2005, 69, 1575-1588.	3.9	145
40	Dodecyl sulfate–hydrotalcite nanocomposites for trapping chlorinated organic pollutants in water. Journal of Colloid and Interface Science, 2004, 274, 613-624.	9.4	171
41	Perrhenate Uptake by Iron and Aluminum Oxyhydroxides:Â An Analogue for Pertechnetate Incorporation in Hanford Waste Tank Sludges. Environmental Science & Technology, 2004, 38, 1765-1771.	10.0	40
42	<i>Ab initio</i> determination of edge surface structures for dioctahedral 2:1 phyllosilicates: implications for acid-base for reactivity. Clays and Clay Minerals, 2003, 51, 359-371.	1.3	135
43	Quantifying surface areas of clays by atomic force microscopy. American Mineralogist, 2002, 87, 780-783.	1.9	74
44	Mercury(II) Sorption to Two Florida Everglades Peats:Â Evidence for Strong and Weak Binding and Competition by Dissolved Organic Matter Released from the Peat. Environmental Science & Technology, 2002, 36, 4058-4064.	10.0	134
45	Structures of quartz (100)- and (101)-water interfaces determined by x-ray reflectivity and atomic force microscopy of natural growth surfaces. Geochimica Et Cosmochimica Acta, 2002, 66, 3037-3054.	3.9	115
46	Nitrate-Cancrinite Precipitation on Quartz Sand in Simulated Hanford Tank Solutions. Environmental Science & Technology, 2001, 35, 4481-4486.	10.0	90
47	Influence of Anionic Layer Structure of Fe-Oxyhydroxides on the Structure of Cd Surface Complexes. Journal of Colloid and Interface Science, 2000, 228, 306-316.	9.4	53
48	Quantification of minor phases in growth kinetics experiments with powder X-ray diffraction. American Mineralogist, 2000, 85, 1217-1222.	1.9	11
49	Surfactant-Templated Mesoporous Silicate Materials as Sorbents for Organic Pollutants in Water. Environmental Science & Technology, 2000, 34, 4822-4827.	10.0	67
50	Evidence for the Formation of Trioctahedral Clay upon Sorption of Co2+ on Quartz. Journal of Colloid and Interface Science, 1999, 220, 181-197.	9.4	80
51	Gibbsite growth kinetics on gibbsite, kaolinite, and muscovite substrates: atomic force microscopy evidence for epitaxy and an assessment of reactive surface area. Geochimica Et Cosmochimica Acta, 1999, 63, 2337-2351.	3.9	56
52	Molecular Modeling of the Tributyl Phosphate Complex of Europium Nitrate in the Clay Hectorite. Journal of Physical Chemistry A, 1998, 102, 6722-6729.	2.5	31
53	All-atom ab initio energy minimization of the kaolinite crystal structure. American Mineralogist, 1997, 82, 657-662.	1.9	82
54	Molecular Controls on Kaolinite Surface Charge. Journal of Colloid and Interface Science, 1996, 183, 356-364.	9.4	273

#	Article	IF	CITATIONS
55	Chemical weathering rate laws and global geochemical cycles. Geochimica Et Cosmochimica Acta, 1994, 58, 2361-2386.	3.9	630
56	Simultaneous precipitation kinetics of kaolinite and gibbsite at 80°C and pH 3. Geochimica Et Cosmochimica Acta, 1993, 57, 4329-4335.	3.9	64